Cement and Concrete Research 41 (2011) 459–466

Contents lists available at ScienceDirect

Cement and Concrete Research

journal homepage: http://ees.elsevier.com/CEMCON/default.asp

Effect of polymer modification of the paste–aggregate interface on the mechanical properties of concretes

Vincent Morin, Mariette Moevus, Isabelle Dubois-Brugger, Ellis Gartner *

Lafarge Centre de Recherche, 38291 St. Quentin Fallavier Cedex, France

ARTICLE INFO

Article history:
Received 16 July 2010
Accepted 12 January 2011

Keywords:
Mechanical properties
Fracture toughness
Polymers
Concrete
Mortar

ABSTRACT

We investigated the effect of thin viscoelastic polymer coatings around aggregate particles on the mechanical properties of "micro-concretes" with a maximum aggregate diameter of 10 mm. Aggregate particles >5 mm were pre-treated with a latex at dosages of up to 2% by mass and dried prior to using the treated aggregate in the micro-concrete mix. Cured prisms were tested in flexion. The results show that thin polymer coatings on aggregates have a significant effect on micro-concrete cracking behaviour at much lower polymer dosages than are commonly used in polymer-modified mortars. We observed a significant improvement in post-peak energy absorption relative to the use of the same amount of polymer dispersed in the bulk paste. But, under the conditions tested here, reductions in the strengths and moduli of the composites due to the polymer additions appear to have more than outweighed the observed positive effects of increases in fracture energy and characteristic length.

1. Introduction

The use of network polymers, such as latexes or resins, to modify the properties of hardened mortars or concretes is not new [1,2]. Examples include resin-impregnated concretes made by polymerization of a monomer absorbed into the hardened concrete, or latex-modified mortars in which a part of the cement paste is replaced by a latex which coalesces during hardening. The polymer serves either to make the product more "flexible" or to reduce its permeability, or both. However, very high polymer dosages, of the order of 10–20% by mass of cement, are usually required in order to obtain a useful effect. Considering the difference in density, this amounts to about 30–60% by volume of cement—a very high dosage. Thus, due to the relatively high cost of polymers, polymer-modified cement products are too expensive for most uses.

It occurred to us that such network polymers might be used more effectively in mortars and concretes if they could be concentrated at the paste/aggregate interface. It was already well known that the paste/aggregate interface has an important role in reducing the brittleness of mortars and especially of concretes, principally by deflecting crack propagation and increasing crack surface area, so we hoped that the use of suitably-tailored polymers designed to absorb energy during crack opening might help to further increase the work of fracture and thus further reduce the brittleness of mortars and concretes, preferably without any negative effect on other properties.

Given that it is difficult to obtain a significant concentration of polymers at the paste–aggregate interface after the polymer has been dispersed into the fresh concrete or mortar, we decided that the best initial approach was to pre-treat the aggregates with polymer so as to ensure that a stable polymer coating of the desired thickness was formed before using the coated aggregates to make mortars or concretes. If a desirable range of polymer properties and coating thicknesses can be found by this simple approach, we believe that it might in the future be possible to find a way of applying such a coating as an integral part of the concrete mixing process.

2. The role of the paste–aggregate interface in the mechanical properties of concrete

Concretes and mortars can for many purposes be treated as two-phase composites composed simply of paste and aggregates. However, if we compare the mechanical performance of any chosen composite of this type with those of its two individual constituents prepared under ostensibly equivalent conditions, we usually find that the maximum stress at rupture for the composite is less than that for either of its two component phases. This reduction in strength is generally attributed to the relative weakness of the paste/aggregate interface, which is difficult to avoid completely, as explained below.

Many microscopists have reported an apparent transition zone, often said to be of the order of 50 μm in thickness, around the aggregates in polished sections of hardened concretes and mortars. This zone appears to have a composition different to that of the

* Corresponding author at: Lafarge Centre de Recherche, 95 rue du Montmurier, 38291 St. Quentin Fallavier Cedex, France. Tel.: +33 474 82 1890; fax: +33 474 82 8011.
E-mail address: ellis.gartner@lafarge.com (E. Gartner).

0008-8846/$ – see front matter © 2011 Elsevier Ltd. All rights reserved.
doi:10.1016/j.cemconres.2011.01.006

average paste composition, in that it has a higher porosity and often also contains large crystal of portlandite [3,4]. This is explained by the "wall-effect," which predicts that there will be fewer large cement (clinker) grains in the zone close to a relatively flat surface during placing; and that, after set and hardening, this will lead to a higher average porosity and also larger pores in which large crystals of relatively mobile phases, such as portlandite, can crystallize. This effect is entirely due to simple considerations of particle packing in the fresh paste before set, and thus should only operate over lengths of the order of the diameters of the particles involved, which is indeed consistent with the microscopic observations on hardened pastes. However, it should not be forgotten that a very significant fraction of the paste falls within 50 μm of an aggregate surface in most concretes and mortars, so the idea that a definite length can delimit what is often referred to as the "ITZ" (Interfacial Transition Zone) makes no real sense. One should perhaps simply say that there is a gradation of paste properties away from the aggregate surface into the paste, but that the highest porosity almost always occurs essentially at the interface itself. This explains the relative weakness of the interface and it is thus normal to imagine that it usually serves as the site for crack initiation and initial propagation in mortars and concretes [5].

Although interfacial defects can never be completely eliminated, there are many ways that one can improve the formulation of concrete so as to minimize their relative importance. These include the following conventional approaches:

1. Reduce the maximum aggregate size and optimize the aggregate particle size distribution: The effect of interfacial defects can certainly be reduced by such an approach, but it has the disadvantage that the resulting mix is generally richer in paste and thus has a lower modulus, greater drying shrinkage, and a greater autogenous temperature rise during curing.
2. Reduce the water/cement ratio of the paste: This decreases the overall paste porosity and increases its strength, which also inevitably increases the strength of the interface. If the average paste strength significantly exceeds the average strength of the aggregates used, then aggregate strength becomes the main factor dictating the strength of the composite, and the relative weakness of the interface with respect to the paste is no longer of great importance. In this case, most cracks tend to pass through the aggregate, rather than around them, which results in a more "brittle" failure.
3. Add well-dispersed ultra-fine particles, such as silica fume, to the paste. Such particles are usually dispersed by high dosages of superplasticizers. Since silica fume is both very fine (<1 μm) and also a reactive pozzolan, it helps to reduce the effect of the interfacial porosity gradient in the fresh paste and subsequently helps fill in the residual porosity with the "most desirable" hydrate phase for bonding (C—S—H) rather than the portlandite that usually forms in pores in ordinary Portland cement pastes. This greatly reduces the weakness of the interface relative to the average paste, although it does not completely eliminate the effect. However, as with the approach of reducing water/cement ratio, if this approach also serves to increase the mean strength of the paste (which is usually the case because of the use of superplasticizers and low water/binder ratios), then aggregate strength again usually becomes the limiting factor.

The application of all three of the above approaches simultaneously is often used in high-performance concretes. The main problem with these approaches is that they lead to concrete embrittlement, because the cracks will tend to pass through the aggregates rather than around them, thus significantly reducing crack surface area and energy absorption during crack propagation [6,7]. This effect can be counteracted by the use of better-quality (stronger) aggregates, in which case the paste–aggregate interface will again become the main locus of crack initiation and initial propagation. Based on the above arguments, it can be seen that the ideal situation would probably be one in which the paste aggregate interface is only very slightly weaker than the average paste, and the average aggregate strength is at least slightly stronger than the average paste. However, if the interface could be further modified so as to absorb more energy during the early stages of crack propagation, it seems likely that the brittleness of the composite could also be further reduced without necessarily reducing its strength.

2.1. Mechanisms of failure

Based on the above discussion, it is reasonable to assume that the principal source of defects in hardened concretes is usually the interface, especially around the large aggregate particles, except in cases where relatively weak aggregates are used (e.g. certain lightweight aggregates) in which case the large aggregates themselves may contain most of the principal defects. But it has also been shown that the presence of aggregates, and even of certain types of voids (preferably spherical voids such as air voids), can also help to stop the growth of cracks by several different mechanisms [8].

- The crack goes around an aggregate that is tougher than the interface. The crack is also to some extent "blunted" by this deviation. In addition, further crack opening must pass around one side of the aggregate, requiring significantly more energy than for simple planar propagation.
- A similar crack-tip blunting effect can occur with an air void, although there is no additional energy absorption added by passage through the void.
- When a crack passes through a zone between two partially debonded aggregates, the local stress intensity is reduced by partial transfer to the aggregate interfaces, and this may be sufficient to stop the growth of the initial crack.

2.2. Potential role of polymers in crack propagation

There are examples in the literature where polymers have been used to modify the matrix-aggregate interface in various types of "concrete." Kim et al. [9] observed that the addition of 2 wt.% of a water-soluble (linear) polyvinyl alcohol in the paste led to a reduction in interfacial porosity, which reinforced the paste–aggregate bond. This type of water-soluble polymer apparently acts as a dispersant and thus allows better packing of fine particles at the interface during mixing.

Network polymers (i.e. polymers cross-linked by either chemical or physical means) with high molecular weights can have high toughness and large extensions at rupture, but they are typically not water soluble and so must be dispersed, e.g. as latexes. Pre-treatment of aggregates with latexes has been used to improve their adhesion to the asphalt matrix in bituminous concretes [10]. Note that pre-treatment of aggregates with paraffin waxes, which do not form strong networks, was shown to reduce both the compressive strength and toughness of some Portland cement concretes [11–13]; but, on the other hand, coating of aggregates with an epoxy-resin that forms a strong, tough network was shown in some cases to strengthen the paste/aggregate interface [11,13,14]. Note also that Rossello et al. confirmed that increasing the paste aggregate bond strength tends to lead to a greater fraction of crack surface area passing through aggregates rather than around them [13,14].

3. Experimental

3.1. Materials

Table 1 shows the formulation of the "micro-concrete" used in the tests. The only variations were in the coarse aggregate, which was

Table 1
Basic micro-concrete formulation.

Constituents	kg/m^3 of concrete
Coarse aggregate (see text for details)	682
0–5 mm Alluvial rounded sand (from Saint Bonnet, France)	724
3–6 mm Crushed sand (from Cassis, France)	232
Limestone filler: BL 200 (Omya Corp.)	83
Cement: CEM I 52.5 N (Ciments Lafarge, Le Havre, France)	375
Defoamer: "Foamaster NYZ"	0.19
Total water: (includes water from latex whenever latex was added)	217.5

either 6/10 mm crushed Cassis limestone (C) or 5/10 mm rounded alluvial silico-calcareous Saint-Bonnet gravel (R).

The latex used to coat the aggregates was BASF's Acronal® S400. This product has a low glass-transition temperature (about −6 °C) and a large elongation before tensile rupture. Details are given in Table 2, taken from the manufacturer's specification sheets.

In the tables of results, the mixes are coded as follows:

- (C) indicating crushed coarse aggregates or (R) indicating rounded coarse aggregates
- (L) = aggregates washed before polymer treatment; (NL) = un-washed before treatment
- (x%) = the mass of dry polymer per mass of dry treated (coarse) aggregate
- (5°) = samples cured and tested at 5 °C (all others cured and tested at 20 °C)
- (T) = control mix (with untreated aggregates)

3.2. Method used to coat the coarse aggregates

We used a commercial 120-litre concrete mixer rotating at 20 rpm and operated with its axis of rotation oriented 30° above the horizontal. With this we were able to treat many different types of aggregate in lots of up to 20 kg. We chose to treat about 20 kg of aggregate per batch (which filled only about 10% of the total volume of the concrete mixer) because this amount enabled us to obtain a homogeneous latex coating over all of the aggregate particles and at the same time to get rapid drying. Typically, 200 g of latex was added to the 20 kg of aggregate in the concrete mixer and the total duration of the coating-drying process was typically 2–3 min. At the end of this process, the 105 °C weight loss of the coated aggregates was <0.5%, indicating a reasonable degree of drying.

3.3. Estimation of the quantity of polymer coating on the aggregates

The amount of polymer coating was measured twice; firstly, immediately after the coating procedure, and secondly, after concrete mixing. Four samples of aggregate (4–6 g each) were taken as a representative sample and then heated in air at 450 °C for two hours. The mass loss expressed as a percentage of the dry mass (averaged over the four samples) was assumed to represent the average percentage polymer coating.

The second measurement was designed to determine the extent to which the coating was removed during concrete mixing. In order to obtain the aggregate samples from micro-concretes, the freshly-mixed micro-concretes were sieved on a 9-mesh size and washed with a large excess of water before being dried at 105 °C for two hours to establish the dry mass, and then heated in air for two hours at 450 °C.

In order to estimate the average thickness of the coating on the treated aggregates, samples of dried treated aggregates from the previous steps were impregnated with an epoxy-resin. After hardening, the mounted samples were polished progressively to obtain a polished section. About ten measurements of coating thickness were made on each polished section, using a binocular microscope with a calibrated length scale, and the results averaged over five separate polished sections to get a reasonably representative value. It was found that a 1% w/w dosage of polymer on the 6/10 mm Cassis aggregate gave a mean coating thickness of 147 ± 66 μm. The high variability of coating thickness is not surprising but the mean thickness is more than twice as high as expected based on the relative volumes of polymer and aggregate used, which suggests that the microscopic averaging procedure is subject to significant errors.

Table 2
Properties of the latex Acronal® S400.

Acronal® S400 (BASF)	
Chemical nature	Anionic dispersion of a copolymer of an acrylic ester and styrene
Elongation at break (method derived from ISO1184-DIN53455)	> 1800%
Tensile strength (N/mm^2).	0.8
Tg °C (DSC)	−6
Surface	Tacky
Average particle size (μm)	0.2

3.4. Preparation and testing of the hardened micro-concretes specimens

For each micro-concrete formulation we cast six 280 × 70 × 70 mm prisms. The specimens were cured at 20 °C in a fog-room for a total of 14 days prior to testing (note: they were demoulded after the first day). All specimens were kept wrapped in a humid cloth during and after removal from the fog room until just before testing, in order to try and prevent any surface drying that might produce micro-cracking. Three un-notched prisms were tested in four-point bending and the other three were sawn at the mid-point to create a groove 7 mm deep and 4 mm wide to function as the crack initiation notch just prior to testing in three-point bending.

Two of the micro-concrete mixes were also cured for 14 days and tested at 5 °C, (after fabrication at 20 °C). The mechanical tests were conducted in a room at 20 °C but the specimens were taken out of the 5 °C curing chamber just before testing and not allowed time to warm up before the test.

3.5. Four-point bending test procedure

The four-point bending tests were done with the geometry shown in Fig. 1, using a span of 210 mm and a spacing, (a), of 70 mm between the two central loading points. The deflection (d) of the upper mid-point was measured with an LVDT placed as shown in the figure. The loading was applied so as to give a constant rate of deflection of 20 μm/min at the upper mid-point. From the linear part of the force-deflection (P vs. D) curve the Young's modulus, E, was calculated using Eq. (1):

$$E = \frac{\Delta P \cdot a}{48\,\Delta d \cdot I}\left[\left(3L^2 - 4a^2\right) + 4.8h^2(1+\nu)\right] \quad (1)$$

where $I = \frac{b h^3}{12}$; b is the width of the prism; h is its height; and ν is its Poisson's ratio.

The flexural strength was calculated from the maximum load (P_{max}) using Eq. (2):

$$f_{fl} = \frac{3P_{max}(L-a)}{2b \cdot h^2} \quad (2)$$

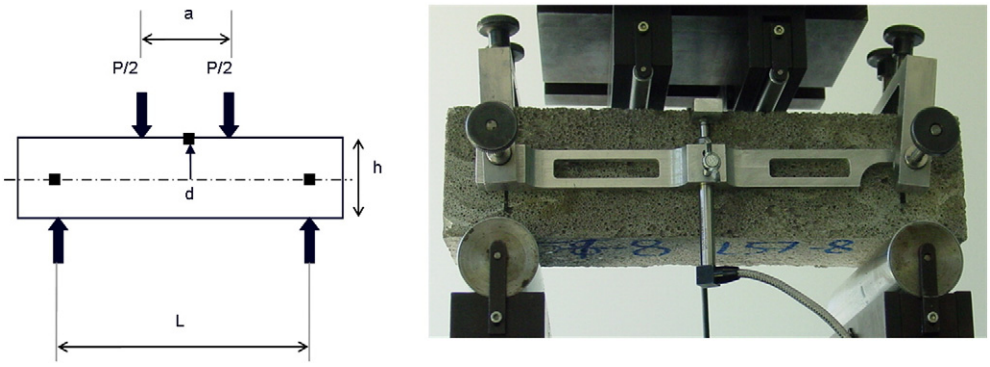

Fig. 1. Four-point bending test set-up.

3.6. Three-point bending test procedure

The three-point bending tests were done with the geometry shown in Fig. 2, also using a span of 210 mm. The crack mouth opening rate was measured with an appropriate detector (CMOD in the figure) and the loading was applied so as to give a constant crack mouth opening rate of 20 μm/min. The calculations were more complex in this case. Firstly, the Young's modulus was calculated from the linear portion of the curve of load (P) vs. crack mouth opening (w) using Eq. (3):

$$E = \frac{3\Delta P \cdot a\,(L-a)}{\Delta w \cdot b\,(h-e)^2} \tag{3}$$

(where e is the initial depth of the notch and a in this case represents the spacing of the CMOD tips).

The tensile strength f_t was taken as the flexural stress at the elastic limit, $\sigma_{fl(el)}$

$$f_t = \sigma_{fl(el)} = \frac{3P_{el} \cdot L}{2 \cdot b\,(h-e)^2} \tag{4}$$

From the flexural stress, σ_{fl}, at any given load, P, we calculated the flexural moment M:

$$M = \frac{\sigma_{fl} \cdot b \cdot (h-e)^2}{6} = \frac{P \cdot L}{4} \tag{5}$$

We could then trace the curve of M vs. $(w - w_{el})$, from the point (w_{el}) at which the M vs. w curve departs from linearity, which corresponds to the creation of a crack. The inverse analysis of this curve by means of the cohesive crack model allowed us to calculate the post-peak σ–w curve for the material.

In order to simplify the description and comparison of these curves of post-peak flexural stress vs. crack mouth opening, we used a bi-linear approximation as shown in Fig. 3. We fitted the two linear sections by a least-squares regression method, which gave us the best fit for the four parameters shown here, defined as follows:

- y_1 is the stress at the departure from elastic behaviour (which is equivalent to the tensile strength, f_t),
- a_1 is the initial post-peak slope,
- w_1 is the limiting crack opening for the initial post-peak slope,
- w_c is the ultimate limiting crack opening at complete failure.

The total fracture energy, G_f, was calculated from the area under the curve, and the characteristic length, L_{ch} was calculated from Eq. (6):

$$L_{ch} = \frac{E \cdot G_F}{f_t^2} \tag{6}$$

Note that this characteristic length was subject to rather large random errors due to the sensitivity of the inverse analysis to small differences in the curve-fitting approximations.

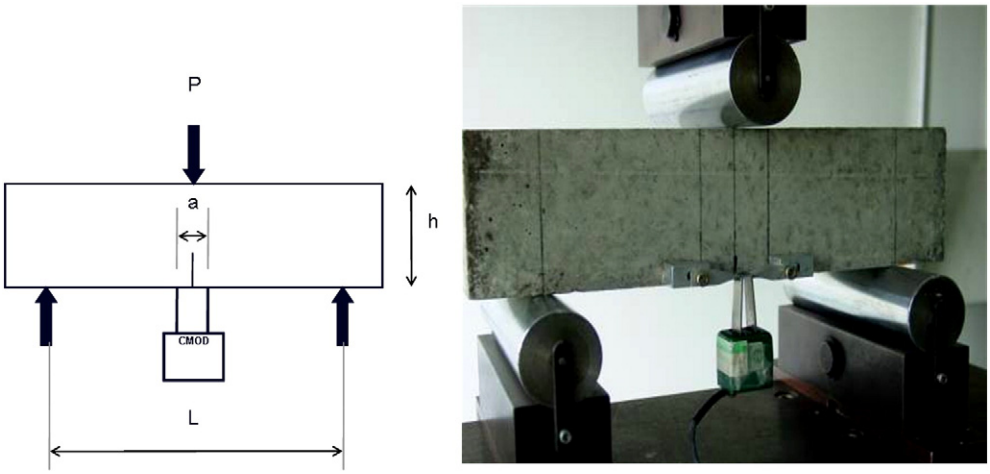

Fig. 2. Three-point loading set-up.

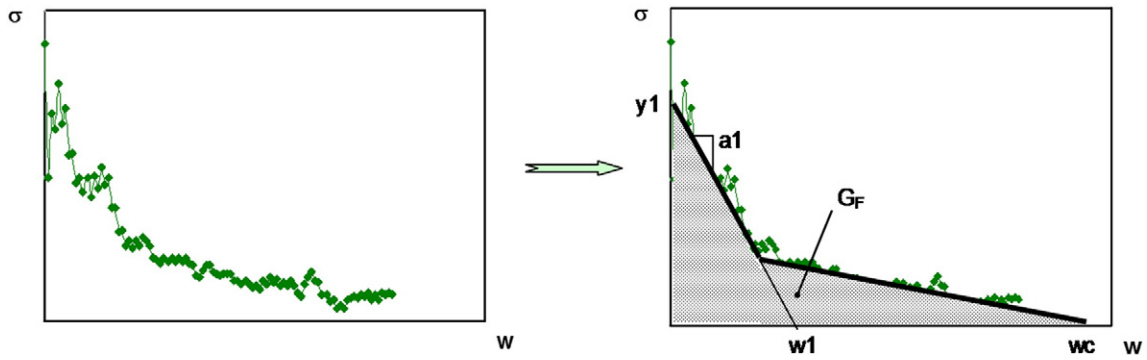

Fig. 3. Bi-linear approximation of post-peak crack opening vs. the flexural stress curve.

4. Results

4.1. Results obtained using the four-point bending test

Fig. 4 shows the results of four-point bending tests on control specimens (four repeats) made with crushed Cassis limestone aggregates, and Fig. 5 shows results for the same aggregates coated with 1% polymer (six repeats). Overall, the repeatability seems good for the control specimens and almost as good for the treated specimens. The results are summarized quantitatively in Table 3. Note that there is a slightly reduced elastic modulus for the mixes cured at 5 °C, as would be expected due to a lower degree of hydration at the lower curing temperature.

Fig. 6 also compares the effect of using the same amount of latex (2% solids by mass of cement, i.e. 1.1% by mass of treated coarse aggregate) in the same mix as used above, but in case (B) the latex was simply added with the mix water (the mix water being reduced accordingly) whereas in case (C) the aggregates were treated as for the other mixes shown in Table 3. The control mix is case (A).

The results in Fig. 6 show a clear difference between the effect of adding the same amount of latex in the form of a coating around the coarse aggregates, as opposed to simply adding it to the bulk paste. When the latex was added to the bulk paste, there was a slight loss of elastic modulus and an earlier deviation from linearity, coupled with a significant drop in the peak load ("modulus of rupture") but no significant increase in post-peak energy absorption (area under the curve after the peak). When the same amount of latex was added as a coating around the coarse aggregates, the deviation from linear elastic behaviour occurred even earlier but the peak load was not much lower than for the bulk paste addition, while the post-peak energy absorption was clearly much higher.

From the results in Table 3, it can be seen that increasing the amount of latex deposited on both types of aggregate tested here significantly decreases the Young's modulus and the flexural strength, but increases the deflection at rupture. Note also that these effects are less marked at 5 °C than at 20 °C, which is presumably due to the fact that the latex used here is considerably stiffer at 5 °C than at 20 °C.

The differences in the effect of 1% latex treatment between crushed and rounded aggregates do not appear to be very significant, despite the fact that microscopic studies of polished sections of the hardened micro-concretes showed that the adherence of the coating to the aggregate during mixing was far worse with the rounded aggregate. Many more detached pieces of latex film were observed in the matrix with the rounded aggregate than with the crushed aggregate. (See examples in Figs. 7 and 8).

4.2. Results obtained on notched micro-concrete prisms subject to 3-point loading

The stress-strain curves obtained during the 3-point loading tests on notched micro-concrete prisms were analyzed by an inversion method allowing the estimation of the following fundamental tensile parameters: f_t (tensile strength), G_f (energy of fracture), and L_{ch} (characteristic length). In comparing these results (Table 4) we can clearly see that increasing the amount of latex greatly reduced f_t but at the same time led to small increases in the energy of fracture and considerably larger increases in the characteristic length. Interestingly, the rounded aggregates gave a lower f_t than the crushed aggregates when tested untreated, but this tensile strength decreased by much less than for the crushed aggregates when treated with 1% latex. The use of a lower curing/testing temperature also decreased the reduction in f_t due to treatment with 1% latex, but didn't seem to reduce the concomitant

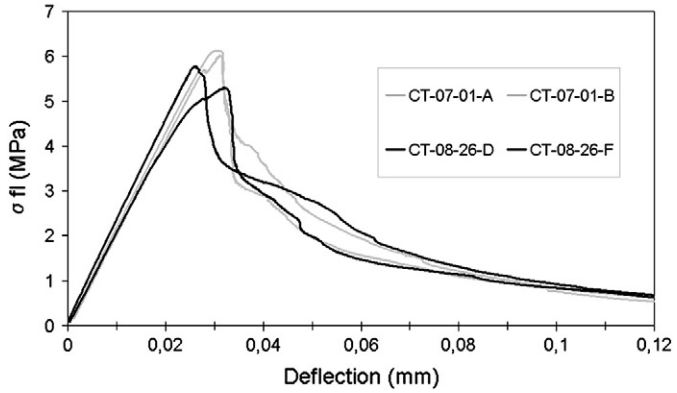

Fig. 4. Comparison of four control micro-concretes made with Cassis aggregates in two separate batches.

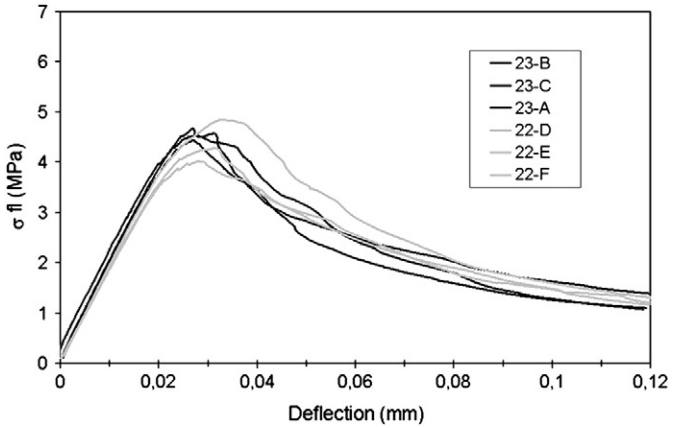

Fig. 5. Comparison of six different mixes containing Cassis aggregates treated with 1% latex.

Table 3
Summary of results of four-point flexural tests.

Mix code	Aggregate type	Washed?	latex (%)	Curing temp.	No of tests	E (GPa)		d_{max} (mm)		f_{fl} (MPa)	
						Mean	SD	Mean	SD	Mean	SD
C-T	crushed	no	–	20 °C	6	36.5	1.6	0.029	0.003	5.7	0.4
C-1%-L	crushed	yes	1%	20 °C	9	31.7	1.7	0.031	0.004	4.7	0.4
C-2%-L	crushed	yes	2%	20 °C	3	23.8	2.6	0.041	0.004	4.1	0.2
R-T	rounded	no	–	20 °C	3	36.5	1.7	0.029	0.002	5.6	0.1
R-1%-L	rounded	yes	1%	20 °C	2	29.3	0.9	0.038	0.004	4.9	0.3
C-T-5°	crushed	no	–	5 °C	2	32.2	0.1	0.030	0.002	5.4	0.4
C-1%-L-5°	crushed	yes	1%	5 °C	3	29.2	0.4	0.035	0.002	5.4	0.2

relative increases in energy of fracture and characteristic length. This suggests that better results could have been obtained by using a latex with a higher glass transition temperature.

In addition to the mechanical test data, we examined fracture surfaces from selected notched prisms broken in three-point bending. An example is shown in Fig. 9. It is apparent that the use of 1% latex in this case significantly increased the fraction of crack surface area going around rather than through the aggregates. This is confirmed by the data in Table 5. We also attempted to assess on which side (paste or aggregate) the latex bond failed preferentially, but it seemed to be fairly evenly distributed.

5. Discussion

The energy, U_S, required for the propagation of a fracture surface is given by Eq. (7):

$$U_S = 2(A_m.\gamma_m + A_a.\gamma_a + A_i.\gamma_i) \quad (7)$$

where A represents the area of the crack of interest and γ represents the specific energy for the creation of new surface for each phase traversed, the subscripts m, a and i, respectively indicating the matrix, aggregate and interface phases, and the factor of two being needed to take into account the fact that both sides of the crack represent new surfaces. If the crack were perfectly flat it would cross all phases simply in proportion to their volume fraction, but in practice, as we have seen, the cracks often pass around the aggregate (through the interfacial phase,) which can increase the crack area (i.e. its roughness) significantly. Now, we may assume for a typical case that the aggregate has the highest fracture energy and the interface has the lowest, i.e. $\gamma_a > \gamma_m > \gamma_i$. In this case, cracks tend to go around the aggregates, but the total energy of fracture can still conceivably be higher than if cracks went through the aggregates because A_i may also increase greatly relative to the area expected based only on volume fraction arguments. Clearly, for any given aggregate properties, as long as the above order of fracture energies is maintained, the energy of fracture of the concrete will increase as γ_i is increased towards the value of γ_m. But if γ_m is then increased towards the value of γ_a, the surface area of the crack will tend to decrease as more cracks go straight through the aggregate, and total fracture energy may well also decrease, leading to embrittlement. Thus, a calculation of crack surface energy can be quite complex, as it depends on the geometry of the system and the distribution and shape of the aggregates as well as simply on the idealized surface energies and volume fractions.

It would be expected that the partial replacement of a "simple" interfacial phase (ITZ) by a polymer phase of very different viscoelastic properties could have a significant effect both on the crack propagation path and on the energy absorbed in the growth of the crack. This is because polymers of the type used here are capable of much larger extensions before rupture than are found in mineral phases. Table 2, obtained from the manufacturer's specifications sheet, states that the polymer used here has an extension at tensile rupture of over 18 times its unloaded length; and its tensile strength is given as being 0.8 MPa, which is only about a factor of 5 lower than the tensile strength of the matrix phase of the micro-concretes tested here. The coating thickness applied to the aggregates here (at the 1% dosage) is estimated to average well over 50 μm. This implies that, if the coatings were properly bonded to both the paste and the aggregate, crack openings of the order of 1 mm would be required in order for the polymer film to fail in tension, which would allow considerable energy absorption during crack opening. But measured critical crack mouth opening displacements during these tests seldom

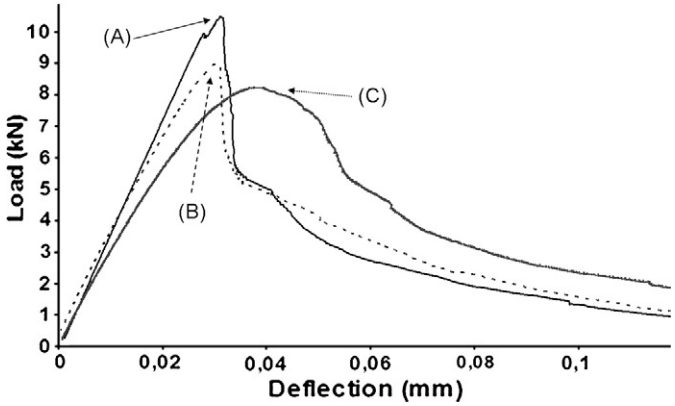

Fig. 6. Effect of latex (2% solids/cement) added in bulk paste (B) or as aggregate coating (C).

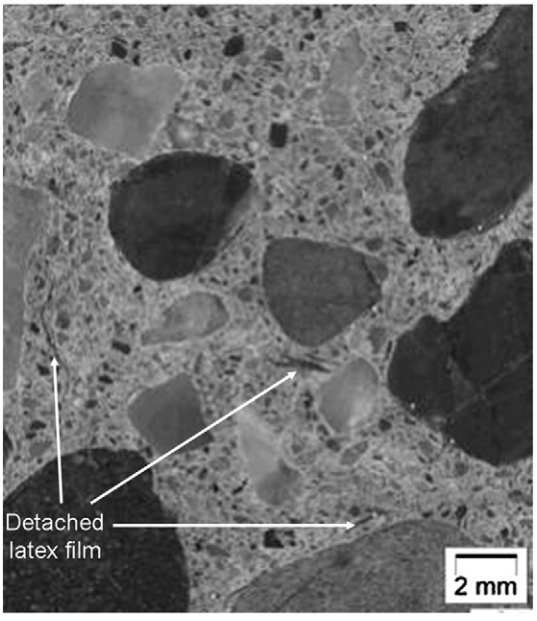

Fig. 7. Polished section of mortar made with unwashed 5–10 mm Saint Bonnet rounded aggregate treated with 1% latex. Note many detached pieces of latex film in the paste matrix.

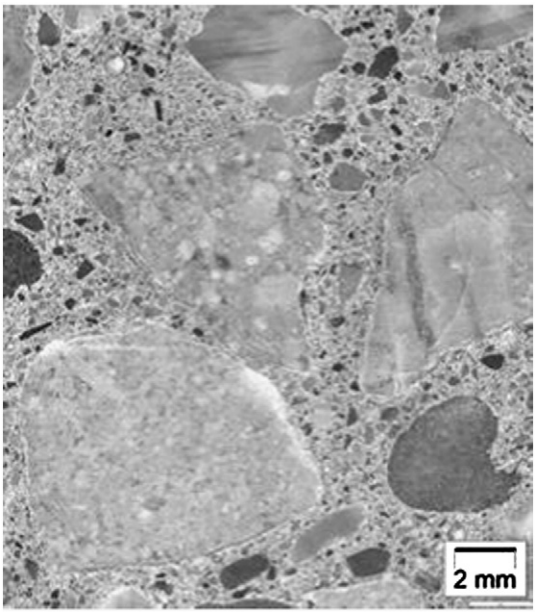

Fig. 8. Polished section of mortar made with unwashed Cassis 6–10 mm crushed aggregate treated with 1% latex. Note that the polymer film appears to have adhered well to the aggregates.

exceeded 150 μm. It thus seems very unlikely that many of the polymer films failed in tension during our tests (at least, those at 20 °C). They presumably mainly failed by de-bonding long before getting close to tensile failure.

The large extensions obtainable with polymers implies that the crack surface energy approach based on Eq. (7) is too simplistic to fully describe the processes involved in the cracking of polymer-modified mineral composites of the type tested here. Due to the very large differences in both elastic moduli and deflections at failure between the polymer and the mineral phases, the post-cracking energy absorption might be increased significantly by viscous dissipation in the polymer if the polymer film thickness were chosen more appropriately and if better bonding could be assured both to the aggregate and to the cement paste matrix. This is very different to the post cracking energy absorption typical of pure mineral composites, where the energy-absorption is generally ascribed to friction.

The fact that somewhat bigger improvements in fracture energy and smaller decreases in strength were observed when the polymer composites were tested at 5 °C suggests that further improvements in performance might be possible if polymer properties and coating thicknesses could be optimized. We do not currently know how to find the optimum conditions, or what level of performance might be ultimately attained because our current micromechanical models are not sophisticated enough to allow us to make such predictions. However, we still believe that simultaneous improvements in the bond between the polymer and the aggregate and between the polymer and the cement paste matrix could lead to significant improvements in the mechanical performance of the hardened composite.

6. Conclusions

The results obtained in this work show clearly that the presence of thin polymer layers at the paste aggregate interfaces in micro-concretes can have a significant effect on cracking behaviour at much lower polymer dosages than are commonly used in conventional polymer-modified mortars where the polymer is simply used in the bulk paste. Unfortunately, under the conditions tested here, the negative effects of reductions in the tensile strengths and Young's moduli of the composites due to the presence of the latex appear to have more than outweighed the positive effects of increases in fracture energy and characteristic length that were also observed. Nevertheless, the prospect of using very small amounts of polymer to improve the toughness of mineral-based composites remains an intriguing possibility. For it to become a practical proposition we must find ways to improve the bonding between the polymers and the mineral phases and also find better micromechanical models for the behaviour of such composites that will allow us to more rapidly estimate the most appropriate polymer properties and coating thicknesses required to maximize composite performance.

Table 4
(a) Results of inverse analysis of 3-point loading tests.

Mix code	Aggregate type	Washed	Latex (%)	Curing temp.	No. of tests	f_t (MPa)		G_f (J/m²)		L_{ch} (mm)	
						Mean	SD	Mean	SD	Mean	SD
C-T	crushed	no	–	20 °C	7	4.9	0.4	72.3	7.4	149	24
C-0.5%-NL	crushed	no	0.5%	20 °C	3	5.0	0.3	68.1	0.7	97	7
C-1%-NL	crushed	no	1%	20 °C	3	2.5	0.5	89.4	7.5	453	159
C-1%-L	crushed	yes	1%	20 °C	7	2.7	0.6	80.1	17.7	293	95
C-2%-L	crushed	yes	2%	20 °C	1	1.9	0.3	84.0	-	500	-
R-T	rounded	no	–	20 °C	3	4.1	0.5	60.4	1.7	132	37
R-1%-L	rounded	yes	1%	20 °C	3	3.3	0.2	71.5	6.4	203	24
R-1%-NL	rounded	no	1%	20 °C	3	3.5	0.9	69.7	12.0	206	145
C-T-5°	crushed	no	–	5 °C	3	4.6	0.3	68.2	7.0	100	10
C-1%-L-5°	crushed	yes	1%	5 °C	3	3.4	0.5	88.7	21.0	229	47

(b) Regression parameters found by bi-linear inverse analysis of 3-point loading tests.

Mix code	Aggregate type	Washed	Latex (%)	Curing temp.	No of tests	a_1 (MPa/mm)		w_1 (mm)		w_c (mm)	
						Mean	SD	Mean	SD	Mean	SD
C-T	crushed	no	–	20 °C	4	103	30	0.030	0.010	0.108	0.005
C-0.5%-NL	crushed	no	0.5%	20 °C	3	106	53	0.027	0.007	0.141	0.037
C-1%-NL	crushed	no	1%	20 °C	3	38	9	0.056	0.008	0.146	0.023
C-1%-L	crushed	yes	1%	20 °C	6	65	19	0.038	0.010	0.157	0.067
R-T	rounded	no	–	20 °C	3	119	19	0.024	0.004	0.095	0.015
R-1%-L	rounded	yes	1%	20 °C	3	57	26	0.041	0.011	0.141	0.019
R-1%-NL	rounded	no	1%	20 °C	3	113	66	0.031	0.022	0.114	0.004
C-T-5°	crushed	no	–	5 °C	3	141	60	0.024	0.009	0.114	0.008
C-1%-L-5°	crushed	yes	1%	5 °C	3	86	23	0.033	0.007	0.140	0.016

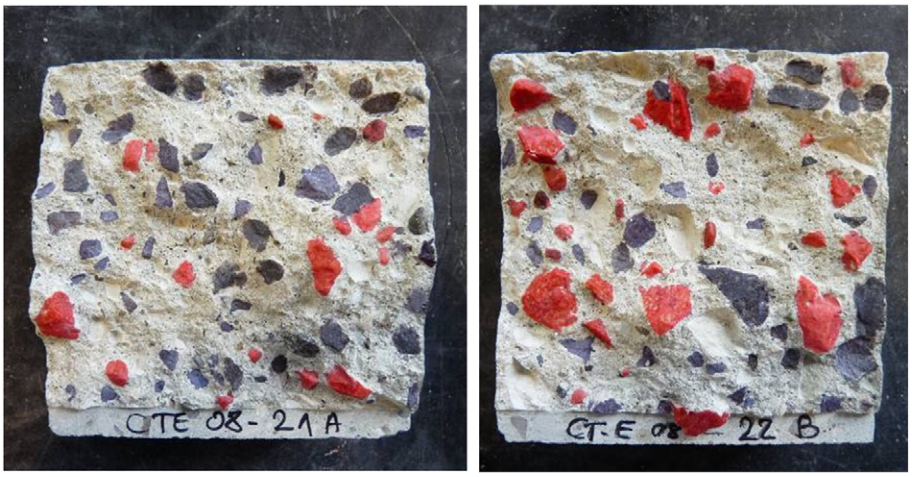

Fig. 9. Fracture surfaces of prisms of micro-concretes C-T (on left) and C-1%-L (on right). Fractured aggregates have been coloured black and aggregates that have pulled out of the matrix have been coloured red.

Table 5
Surface area fractions of fractured aggregates (S_f/S_{tot}) and pulled out aggregates (S_p/S_{tot}) for four specimens.

Mix Code	Specimen	S_f/S_{tot}	S_p/S_{tot}
C-T	CT-08-21-A	12%	5%
C-1%-L	CT-08-22-B	9%	11%
C-T	CT-08-21-D	12%	nm
C-1%-L	CT-08-23-A	7%	nm

Acknowledgements

We would like to thank Stephane Rigaud, Florence Serre, Fabienne Begaud and Hubert Bally for assistance with various aspects of this work.

References

[1] A. Blaga, J.J. Beaudoin, Le béton modifié aux résines, *Digests de la construction au Canada,* CBD-241-F, 1986.
[2] ACI Committee 548, State of the art report on polymer modified concrete. *ACI 548, 3R-91*, 1991.
[3] K. Scrivener, A.K. Crumbie, P. Laugesen, The Interfacial Transition Zone (ITZ) between cement paste and aggregate in concrete, Interface Sci. 12 (2004) 411–421.
[4] A. Bascoul, Formation des microfissures, Ann. IBTP (No. 398) (1981).
[5] J.C. Maso, La liaison pâte-granulats in "Le béton hydraulique", Presses de l'ENPC, Paris, 1982.
[6] J.C. Maso, Influence of the interfacial transition zone on composite mechanical properties, in: J.C. Maso (Ed.), Interfacial Transition Zone in Concrete, RILEM Report 11, , 1996, pp. 103–116.
[7] L. Sorelli, G. Constantinides, F.J. Ulm, F. Toutlemonde, The nano-mechanical signature of Ultra High Performance Concrete by statistical nanoindentation techniques, Cem. Conc. Res. 38 (No. 12) (2008) 1447–1456.
[8] S.P. Shah, F.J. McGarry, Griffith fracture criterion and concrete, J. Eng. Mech. Division Proc. ASCE (1971) 1663–1676.
[9] J.-H. Kim, R.E. Robertson, A.E. Naaman, Structure and properties of poly(vinyl alcohol)-modified mortar and concrete, Cem. Conc. Res. 29 (1999) 407–415.
[10] R.-F. Ju, Y.-L. Lee, S.H. Lin, W.J. Burke, Surface modification of aggregate in asphalt concrete, Colloids Surf. 49 (1990) 395–399.
[11] G.V. Guinea, K. El-Sayed, C.G. Rocco, M. Elices, J. Planas, The effect of the bond between the matrix and the aggregates on the cracking mechanism and fracture parameters of concrete, Cem. Conc. Res. 32 (2002) 1961–1970.
[12] G. Prokopski, J. Halbiniak, Interfacial transition zone in cementitious materials, Cem. Conc. Res. 30 (2000) 579–583.
[13] C. Rossello, M. Elices, Fracture of model concrete—1/ type of fracture and crack paths, Cem. Conc. Res. 34 (No. 8) (2004) 1441–1450.
[14] C. Rossello, M. Elices, G.V. Guinea, Fracture of model concrete—2/ Fracture energy and characteristic length, Cem. Conc. Res. 36 (No. 7) (2006) 1345–1353.